



Available online freely at www.isisn.org

Bioscience Research

Print ISSN: 1811-9506 Online ISSN: 2218-3973

Journal by Innovative Scientific Information & Services Network



RESEARCH ARTICLE

BIOSCIENCE RESEARCH, 2021 18(3): 2416-2422.

OPEN ACCESS

Antioxidant activity of cobalt and Magnesium Nanoparticles synthesized by *Nigella Sativa* seeds extract

Syeda Hajira Shah, Farhad Ali, Tahir Salam and Asma

Institute of Biotechnology and Microbiology, Bacha Khan University Charsadda, Pakistan

*Correspondence: drfarhad@bkuc.edu.pk Received 29-03-2021, Revised: 16-09-2021, Accepted: 18-09-2021 e-Published: 19-09-2021

The present study was aimed at green synthesis of eco-friendly cobalt and magnesium nanoparticles using aqueous extract of *Nigella Sativa* seeds. The high biological activity of cobalt and its nanoparticles have an extensive range of applications. The healthy *nigella sativa* seeds were collected from herbal shop in district Charsadda. Cobalt and Magnesium, nano-particles have been characterized by numerous techniques such as XRD, FTIR, SEM, UV and were analyzed for their antioxidant activity. The presence of cobalt and magnesium were confirmed from the EDX of the nanoparticles. The carbon was present in large quantity due to the presence of *nigella* extract which were organic in nature. FTIR analysis gave confirmation about capping of Cobalt and Magnesium nanoparticles and furthermore evaluated that reduction done by phenolic, carboxyl and hydroxyl groups while stabilization components of Cobalt and Magnesium nanoparticles were amide linkage and amino acid. SEM Micrographs showed that particles of Co are agglomerate and uniform in morphology while Mg are dispersed. The XRD peak gave information about the phase purity, size, internal crystalline structure and nature of the synthesized NPs. The synthesized Cobalt-oxide NPs were 26nm and cubic shaped while Mg NPs were crystalline in structure with an average size of 45nm. It was also concluded that antioxidant activity of Co NPs was higher than Mg NPs. Further research on Co and Mg NPs is needed to explore its environmental application.

Keywords: *Nigella sativa*, seeds extract, Cobalt nanoparticles, Magnesium Nanoparticles, FTIR, UV, SEM, EDX and XRD.

INTRODUCTION

Nanotechnology is “the design, characterization, imaging, modeling, application of structures, manipulating matter and production of systems and devices by controlling shape and size at nanometer scale” (Alexandre Albanese et al). The term ‘Nano’ is derived from Greek word for ‘dwarf or miniature size’ which is used to indicate one billionth of a meter (Sangamithra and Thirupathi, 2009). Nanoparticles are materials ranging in size from 1 -100 nm that due to their size may differ from the bulk material. Presently, different metallic nano-materials are being produced using Copper, Zinc, Cobalt, Titanium,

Magnesium, Gold, Alginate and Silver, exhibited their own structural properties and important biological activities (Dubchak et al.). Nanoparticles have increased surface area and small size hence used in drug delivery for treatment of breast cancer, head and neck cancer, bio informatics and antibacterial agent to eliminate multidrug resistant strains. Nanoparticles are used as antibacterial agent in food technology, textile coating, environmental cleaning water disinfection (Jaworek, et al. 2008). Among these metal nanoparticles Cobalt and Magnesium are most widely recognized for their applications in medical and scientific field (Puntès et al. 2001). Cobalt

nanoparticles are more focused for human healthcare due to its antiseptic action. Cobalt nanoparticles have strong antibacterial activity, they are lipophile and able to cross cell membrane to interfere intracellular reactions of microbes (Ladan et al. 1993). Similarly, magnesium nanoparticles are another essential element used in agriculture. They exhibit strong antimicrobial activity toward the pathogenic bacteria, fungi and few viruses. MgNPs are nontoxic to human, therefore they have been recognized as safe materials by the United States Food and Drug Administration (Krishnamoorthy, et al. 2012). Various techniques are used for synthesis of NPs. Traditionally most of the metal NPs were synthesized by chemical and physical methods. Some of the commonly used chemical methods are sol-gel technique, microemulsion technique, hydrothermal synthesis, polyol synthesis and chemical vapor synthesis. However, these methods are costly, toxic, and hazardous and required difficult separation procedure (Brinker, and Seherer). Alternatives to Chemical and physical methods are Biological methods of nanoparticles synthesis using microorganisms, enzymes, fungus, plants and their parts. (Shankar et al. 2004 and Ahmad et al. 2011). Biosynthesis of NPs using plants extract is one of the most effective, clean, convenient, less time consuming, ecofriendly, nontoxic and simple method (Iravani, 2011). Reduction properties to reduce metal ions to their corresponding nanoparticles and capping properties for protection both are present in the plant. The major advantages of synthesizing nanoparticles using plants extracts could be related to the absence of any complex processes such as complicated purification steps and maintenance of the microbial cell culture (Narayanan and Sakthivel, 2011). Among different plants *Nigella sativa* is reported to exhibit strong antimicrobial activity against *Salmonella typhi*, *Pseudomonas aeruginosa*, *H. Pylori* and *Escherichia coli* but more sensitive against Gram-positive bacteria such as *Staphylococcus aureus* and *Vibrio cholera* and their extracts can be used for synthesis of nanoparticles.

MATERIALS AND METHODS

3.1 Plant material processing

The plant seeds were locally collected from Charsadda, Khyber Pakhtunkhwa, and were identified in Dept. of botany, Bacha Khan University, Charsadda. Plant seeds were washed completely and powdered by grinding the plant

seeds using electric grinder. 50 g powder was added into 500 ml flask and boiled by adding 500 ml distilled water for 20 mins at 150°C. The powder was incubated overnight at 37°C for maximum extraction. Filtration was done with the help of Whatman filter paper and the extract was stored at 4°C until further use.

3.2 Biosynthesis of CoO-NPs

CoO-NPs were synthesized by the protocols reported by Khalil et al. (2017a) with minor modifications [19]. Briefly, 3.0 g of CoCl_2 was added to 100 ml plant extract in 500 ml flask. The solution was gently stirred for 2 hours at 60°C. Initial color change from marron to plum color was observed. To collect CoO-NPs, the solution was first cooled down, which was then followed by centrifugation for 12 mints at 6500 rpm. The supernatant was discarded while pellets were subjected to washing three times with distilled water. The resulting precipitates after washing were calcinated at 500°C for 2 hours to remove water content and any plant residue.

3.3 Biosynthesis of (MgO)NPs

The synthesis of MgO-NPs was achieved through protocols reported by Khalil et al. (2017b) with minor modifications [20]. 100 ml Plant extract was added to 3.0 g MgSO_4 salt. The solution was kept on hot plate stirrer at 85°C for 2 hours. Initial color change from olive green to orange indicated synthesis of MgO-NPs. For separation of MgO-NPs, the mixture was cooled and then centrifuged for 12 min at 12,000 rpm. Supernatant was then removed, and the pellets were washed three times with distilled water. The resulting precipitates after washing were calcinated at 500°C for 2 hrs to remove water content and any plant residue.

3.4 Characterization of CoO and MgO Nanoparticles

3.4.1 Fourier Transmission Infrared Spectroscopy (FTIR)

The crude suspension of CoO and MgO NPs was initially centrifuged at 12000 rpm for 15 min to remove the unwanted impurities. The pellet was re suspended in the ethanol and was again centrifuged at 12000 rpm for 15min to further remove the impurities. The procedure was repeated twice. Final pellet obtained was washed with deionized water to get the pure CoO and MgO NPs. The sample was completely air dried at

room temperature. The collected powdered of CoO and MgO-NPs were taken for FTIR analysis.

3.4.2 X-Ray Diffraction (XRD)

The crystalline nature of green synthesized of CoO and MgO NPs was confirmed by XRD pattern. The XRD data were recorded using Panalytical X'Pert X-ray diffractometer using $\text{CuK}\alpha$ ($\lambda = 1.54056 \text{ \AA}$).

3.4.3 Scanning Electron Microscopy (SEM)

The synthesized CoO and MgO-NPs were monitored morphologically using SEM (ZEISS-EVO MA 15, Japan). A thin film of each synthesized CoO and MgO-NPs sample was prepared by dropping a small amount on the grid.

3.4.4 Characterization of Nanoparticle by Energy Dispersive X-RAY Spectroscopy

Energy Dispersive X-Ray Spectroscopy (EDX) is a technique which provides information about the elemental composition of a sample in the form of curve output. This analytical technique is generally used in conjunction with the SEM. EDX technique bring about characterization of elemental composition of sample by detecting the X-ray emitted from the sample during the process of bombardment (by an electron beam). EDS X Sight Oxford instrument was used for EDX analysis.

3.5 Biological applications:

3.5.1 Antioxidant assays

3.5.2 Total antioxidant capacity determination (TAC):

The assay was employed to examine the total antioxidant capability of the sample. In the experiment, 100 μL of sample was added to the Eppendorf tubes with the help of micropipette. After that, 900 μL of TAC reagent (0.6 M Sulphuric acid, 28 mM sodium phosphate and 4 mM ammonium molybdate, in 50 mL dH_2O) was transferred to Eppendorf tubes containing the tested samples. The reaction mixture was placed in water bath for incubation at 90°C for 2.5 hrs, followed by cooling at room temperature. Absorbances of the samples were then measured at 630 nm through a microplate reader. The experiment was performed three times. TAC was expressed as μg ascorbic acid equivalent (AAE) per mg of the sample.

Total reducing power determination (TRP)

The procedure was used in triplicate to check the total reducing power of the sample. Test sample (100 μL) along with 400 μL of 0.2 Molar phosphate buffer (pH 6.6) and potassium ferric cyanide (1% w/v) was added to the Eppendorf tubes followed by incubation in water bath at 55°C for 30 min. Subsequently, 400 μL of trichloroacetic acid (10% w/v) was added to each Eppendorf tube followed by centrifugation for 10 min at 3000 rpm. The supernatant (140 μL) of each mixture was poured into corresponding wells of a 96-well plate already containing 60 μL of ferric cyanide solution (0.1% w/v). Absorbance of the samples was then recorded using microplate reader at 630 nm. The same procedure, as mentioned earlier was followed both for positive and negative controls. TRP was expressed as μg AAE (ascorbic acid equivalent) per mg the tested sample.

3.5.4 Free radical scavenging assay (FRSA)

The possible free radical scavenging ability of Cobalt and Magnesium NPs were investigated for their antioxidant potential using DPPH reagent at concentrations ranging from 12.5 μL to 400 μL . Tested samples (10 μL) was added to each well of a 96 well plate. DPPH reagent (190 μL) was then transferred to every well having the sample. It was then incubated in dark for 60 minutes at 37°C . Ascorbic acid was used as positive control and DMSO was employed as negative control. Absorbance of reaction mixture was measured at 515 nm using a microplate reader and free radical scavenging potential was measured in percentage using the following equation

$$(\%) \text{ FRSA} = \left(1 - \frac{Abs}{Abc}\right) \times 100$$

Where Ab_c and Ab_s indicates the absorbance of negative control and sample, respectively.

3.5.5 ABTS Assay

ABTS scavenging activity was evaluated using ABTS assay (also known as Trolox antioxidant assay) with minor modification. ABTS reaction solution was prepared by mixing potassium per sulphate (2.45 mM) with 7 mM ABTS salt in equal proportion followed by incubation for 16 hrs in dark. After mixing with test samples, the final reaction mixture was replaced in dark for 15 min at 25°C . Absorbance of the test samples was recorded at 734 nm via Microplate reader (BioTek ELX800). Trolox and DMSO was used as positive and negative controls, respectively. The Antioxidant potential of the

samples was expressed as TEAC and the assays was executed in triplicates.

RESULT AND DISCUSSION

4. Characterization of CoO and MgO Nanoparticles

4.1 Band gap of nanoparticles

The band gap of nanoparticles was found by performing UV of the particles. The two synthesized nanoparticles showed good band gap. The band gap of CoO-NPs was 3.3eV, while for the MgO-NPs, it was 3.5eV as shown in fig. (a,b). The smaller band gap showed good activity due to which electron transfer from valence band to conduction band which decreased excitation of electrons.

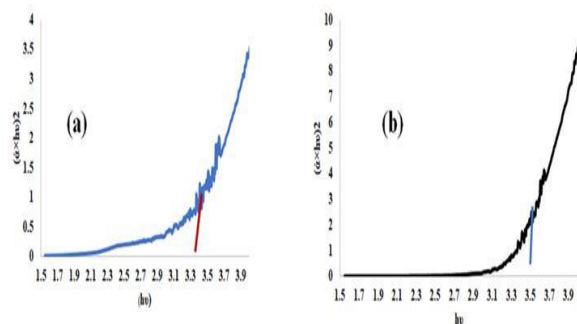


Figure 4.1: (a) The band gap of Co₃O₄ (b) The band gap of MgO

4.2 Fourier transform Infrared spectroscopy (FT-IR)

The FTIR spectra of Co, Mg shown in Figure 4. The main characteristic peaks at 1000 cm⁻¹ and 1200 cm⁻¹ (C–O stretch), 1650 cm⁻¹ (C=O stretch and N–H bending), were observed.

The FTIR spectrum of a CoO and MgO nanoparticle showed in the two infrared absorption peaks revealed the vibrational modes of Co, Mg nanostructures in the range of 586 cm⁻¹ which clearly confirmed the formation of metal oxide nanoparticles. Similarly in previous studies FTIR spectrum analysis was performed to detect the presence of organic compounds in *E. tirucalli*, which could be responsible for reducing and stabilizing metal ions to form nanoparticles. The FTIR spectrum wavenumber for both MgONPs and CoONPs was between 500 and 4000 cm⁻¹ and the NPs were annealed at different temperatures to establish the presence and absences of different vibrations (Kgosiemang et

al. 2020).

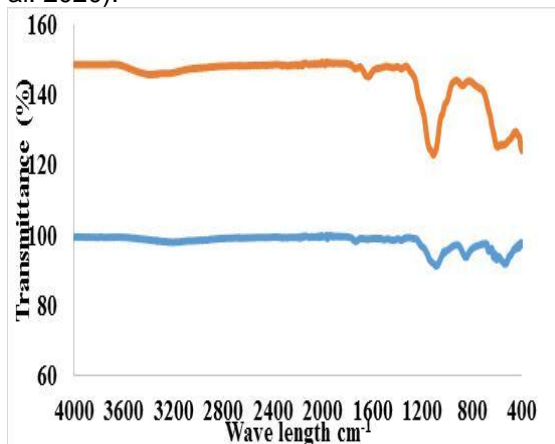


Figure 4.2: (a) FT-IR spectra Of Co₃O₄ and (b) MgO nanoparticles.

4.3 X-ray diffraction analysis (XRD)

The XRD analysis of Co₃O₄ NPs is shown in Figure 1a. The Co₃O₄ NPs XRD resulted in numerous weak peaks, positioned at 2theta values of 21.16, 26.93, 29.24, and 36.45, which correspond with the plane metallic cobalt indices of (111), (201), (100), and (112)(220), Co₃O₄ cubic structure. The size of Cobalt Oxide was calculated 26nm.

While the MgO NPs as shown in Fig. 1(b) clearly exhibits the peaks at angles 18.57°, 38.02°, 46.98°, 64.36, and 78.66° corresponds to (111), (220), (222) and (311) planes (JCPDS No. 87-0653), which revealed the formation of polycrystalline crystalline structure of MgO NPs. No other impurity phase was found in the XRD pattern. XRD pattern showed high intensity (0 0 2) orientation peak revealing the high crystallinity of the synthesized material. The mean crystallite size is calculated using (0 0 2) reflection and found to be 45 nm. Similarly in previous studies The XRD results for CoONPs and MgONPs demonstrated various peaks confirming the formation of metal-ion crystals. The XRD patterns for MgONPs observed showed peaks at 2θ values of 36.8, 42.9, 62.0, 74.0 and 78.1, which correspond to metal crystalline (111), (200), (220), (311) and (222), respectively (Venkatesha et al. 2013; Xu et al. 2018 and Kgosiemang et al. 2020).

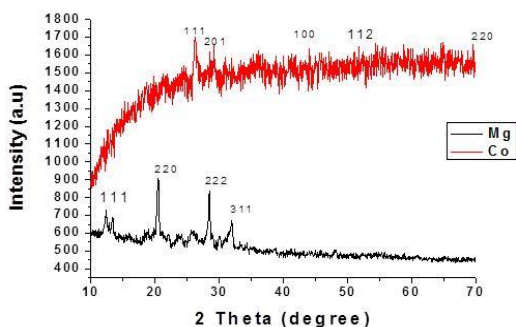


Figure 4.3: (a) XRD spectra of Co_3O_4 and (b) MgO NPs

4.4 Scanning electron microscopy (SEM)

The SEM images of both Co_3O_4 and MgO are shown in fig. 2. SEM micrographs Co_3O_4 revealed agglomerated uniform morphology while MgO were dispersed. In contrast previous studies also perform SEM imaging to analyze the morphological character and provide more details on the size of the synthesized MgONPs and CoONPs. The distribution of the MgONPs was in a uniform network-like agglomerated form. While CoONPs in dispersed form (Wang et al. 2005; Pattanshetti, 2018).

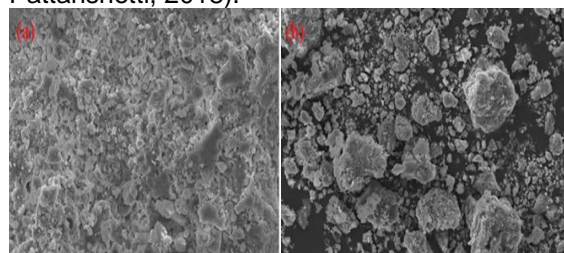


Figure 4.4: (a) Co_3O_4 (b) MgO NPs

4.5 Energy dispersive X-ray analysis

The presence of Cobalt and Magnesium nanoparticles was confirmed from the EDX of the nanoparticles. The EDX composition showed that Cobalt and Magnesium were present in large quantities. The presence of oxygen clearly confirmed the presence of metal Oxide nanoparticles. The carbon was present in large quantities due to the presence of nigella extract which were organic in nature. The presence of Carbon, Nitrogen, Sodium, Aluminum, Sulphur, Potassium and iron were also present in the plant extract.

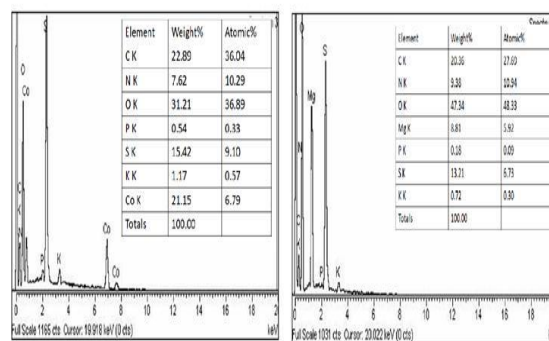


Figure 4.5: (a) EDX spectra of Co_3O_4 and (b) MgO

4.6 Antioxidant activity

The in vitro antioxidant potential of Co_3O_4 -NPs and MgO-NPs was screened using total antioxidant capacity (TAC), total reducing power (TRP), ABTS (2,2'-azino-bis (3-ethylbenzothiazoline-6-sulfonic acid) and DPPH (2, 2-diphenyl-1-picrylhydrazyl) free radical scavenging assays (FRSA). The results are illustrated in Table-2. Highest Antioxidant activity was observed as 82.12 ± 0.28 μg AAE/mg for Co_3O_4 -NPs at $400 \mu\text{g}/\text{mL}$ against ABTS, while MgO-NPs showed comparatively less ABTS activity of 72.14 ± 0.38 μg AAE/mg. Highest antioxidants capacity in terms of ascorbic acid equivalents was observed as 62.1 ± 0.83 μg AAE/mg for Co_3O_4 -NPs at $400 \mu\text{g}/\text{mL}$ while MgO-NPs showed comparatively less TAC activity of 60.39 ± 0.62 μg AAE/mg. TAC assay was supported with total reducing power estimation (TRP) technique. In the current study, highest TRP was observed as 55.52 ± 0.71 μg AAE/mg for MgO -NPs while Co_3O_4 -NPs displayed weak reducing potential of 46.41 ± 0.83 μg AAE/mg. Moreover, DPPH free radical scavenging assays were also employed. In the study, excellent free radical scavenging activities of Co_3O_4 -NPs and MgO-NPs was observed. Highest DPPH free radical scavenging activity for Co_3O_4 -NPs was calculated as $77.3 \pm 0.28\%$ and $61.4 \pm 0.12\%$ for MgO-NPs. From the results summarized, it was concluded that the biosynthesized NPs displayed excellent antioxidant potential, particularly Co_3O_4 -NPs when compared to MgO-NPs. Tayyaba Shahzadi et al. (2019) synthesize economical safe cobalt nanoparticles by using *Celosia argentea* plant extract and evaluated their antioxidant activity. She concluded that the synthesized CoNPs donate electrons or hydrogen to a highly stable DPPH free radical. Hydroxyl free radical is

a powerful reactive oxygen species which damage plasma membrane and results in cell death. In her work it was observed that 80% DPPH was degraded by taking concentration of CoNPs above 500µg/ml. while, in our current research, 77% of DPPH was degraded by using 400µg/ml of CoNPs. Sushma, N. J et al (2016) synthesized Magnesium oxide nanoparticles (MgO-NPs) by using whole plant extract of *Clitoria ternatea*. Antioxidant activity of CoNPs was assessed by Diphenylpicrylhydrazyl (DPPH) Free radical scavenging activity. In this work 50–150 µl (1 mg/ml) of crude extract of the plant was tested and compared with standard ascorbic acid. The plant showed the maximum antioxidant activity which is almost similar to standard. It was noted that the biologically synthesized MgO-NPs has 65 % maximum inhibition activity. This maximum inhibition of *Clitoria ternatea* synthesized MgO-NPs may be due to the bioactive components present in the plant extract. Powder form of MgO-NPs were dissolved in distilled water and added to 1ml DPPH. The mixture was shaken well and incubated for 30 min at room temperature and absorbance was measured at 517 nm in a spectrophotometer. Comparing it with our experiment absorbance of reaction mixture was measured at 515 nm using a microplate reader and free radical scavenging potential was measured in different percentages.

NPs	Conc (µg/mL)	TAC (µg AAE/mg)	TRP (µg AAE/mg)	ABTS (CTEAC)	DPPH (%FRSA)
Co	400	62.1±0.83	46.41±0.83	82.12±0.28	77.3±0.28
	200	41.37±0.27	39.51±0.87	76.63±0.39	62.1±0.71
	100	38.86±0.72	22.23±0.26	50.64±0.56	55.69±0.32
	50	25.29±0.76	25.76±0.58	42.47±0.26	40.45±0.98
	25	17.16±0.25	20.41±0.36	33.39±0.15	32.19±0.48
Mg	400	60.39±0.62	55.52±0.71	72.14±0.38	61.4±0.12
	200	43.37±0.27	47.6±0.18	55.63±0.98	55.9±0.73
	100	31.47±0.52	35.29±0.67	44.64±0.56	41.25±0.59
	50	26.29±0.47	26.16±0.52	32.47±0.16	29.38±0.18
	25	18.21±0.73	18.16±0.51	20.39±0.15	20.89±0.64

CONCLUSION

It is concluded from our results that green synthesis of cobalt and magnesium NPs was successfully carried out by using *Nagilla sativa* seeds' aqueous extract, which indicated *Nagilla sativa* could potentially be used as an effective reducing and capping agent for biological

synthesis of Co and Mg NPs. The biosynthesized Cobalt and Magnesium NPs were characterized using UV, FTIR, XRD, SEM and EDX. The band gap of nanoparticles was found by performing UV-Vis spectroscopy. Both synthesized nanoparticles showed good band gap. Smaller band gap was observed for Co, while for the Mg the band gap observed was comparatively larger. FTIR analysis verified the existence of phytochemicals involved in the transfer of metallic ions to NPs. SEM Micrographs showed that nanoparticles of Co are agglomerate and uniform in morphology while, Mg are dispersed. Maximum Antioxidant activity was observed for Co nanoparticles at 400µg which was 82.12 against ABTS while minimum antioxidant activity was observed for Mg nanoparticles at 25 µg which was 20.39% against ABTS. Moreover, it was also concluded that out of the two synthesized NPs, cobalt showed better antioxidant activity. Further, these nanoparticles were evaluated for their antioxidant activity and showed higher antioxidant activity compared to extract.

The significance of this study demonstrated a broad range of applications of synthesized nanoparticles.

CONFLICT OF INTEREST

The authors declared that present study was performed in absence of any conflict of interest.

AUTHOR CONTRIBUTIONS

SHS performed the experiments and wrote the manuscript, FA designed the experiments, edited the manuscript. TS helped in data analysis and A helped in manuscript write up.

Copyrights: © 2021@ author (s).

This is an open access article distributed under the terms of the [Creative Commons Attribution License \(CC BY 4.0\)](https://creativecommons.org/licenses/by/4.0/), which permits unrestricted use, distribution, and reproduction in any medium, provided the original author(s) and source are credited and that the original publication in this journal is cited, in accordance with accepted academic practice. No use, distribution or reproduction is permitted which does not comply with these terms.

REFERENCES

- A. Jaworek and A. T. Sobczyk, *J. electrost.*, 2008, 66, 1 97-219. Ahmad N., Sharma S., Singh V.N., Shamsi S.F, Fatma A. and Mehta B.R., Biosynthesis of silver nanoparticles from

- Desmodium triflorum : a novel approach towards weed utilization, *Biotechnol. Res. Int.* 454090 (1-8), (2011)
- Alexandre Albanese, Peter S. Tang, and Warren C.W. Chan. The Effect of Nanoparticle Size, Shape, and Surface Chemistry on Biological Systems. *Annual Review of Biomedical Engineering* 2012, Vol.14:1-16
- Dubchak S., Ogar A., Mietelski J.W. and Turnau K., Influence of silver and titanium nanoparticles on arbuscular mycorrhiza colonization and accumulation of radiocaesium in *Helianthus annuus*, *Span. J. Agric. Res.*, 8(1), 103-108, (2010).
- Kgosiemang, I. K., Lefojane, R., Direko, P., Madlanga, Z., Mashele, S., & Sekhoacha, M. (2020). Green synthesis of magnesium and cobalt oxide nanoparticles using *Euphorbia tirucalli*: Characterization and potential application for breast cancer inhibition. *Inorganic and Nano-Metal Chemistry*, 50(11), 1070-1080.
- Krishnamoorthy, K., Moon, J. Y., Hyun, H. B., Cho, S. K., & Kim, S. J. (2012). Mechanistic investigation on the toxicity of MgO nanoparticles toward cancer cells. *Journal of materials chemistry*, 22(47), 24610-24617.
- Ladan, H., Nitzan, Y., & Malik, Z. (1993). The antibacterial activity of haemin compared with cobalt, zinc and magnesium protoporphyrin and its effect on potassium loss and ultrastructure of *Staphylococcus aureus*. *FEMS microbiology letters*, 112(2), 173-177.
- Narayanan KB, Sakthivel N (2011) Green synthesis of biogenic metal nanoparticles by terrestrial and aquatic phototrophic and heterotrophic eukaryotes and biocompatible agents. *Adv Colloid Interface Sci* 169:59–79 .
- Pattanshetti, V. V.; Shashidhara, G. M.; Veena, M. G. Dielectric and Thermal Properties of Magnesium Oxide/Poly(Aryl Ether Ketone) Nanocomposites. *Sci Eng. Compos. Mater.* 2018, 25, 915–925. DOI: 10.1515/secm-2016-0273.
- Puntes, V. F., Krishnan, K. M., & Alivisatos, A. P. (2001) Colloidal nanocrystal shape and size control: the case of cobalt. *Science*, 291(5511), 2115-2117.
- S. Irvani, *Green Chem*, 2011, 13, 2638-2650.
- Sangamithra, A., & Thirupathi, V. (2009). Nanotechnology in food. *Science Tech Entrepreneur E-zine*, January. <http://www.technopreneur.net/informationdesk/sciencetechmagazine/2009/jan09/nanotechnology.pdf>
- Erişim, 20, 2011
- Shahzadi, T., Zaib, M., Riaz, T., Shehzadi, S., Abbasi, M. A., & Shahid, M. (2019). Synthesis of Eco-friendly Cobalt Nanoparticles Using *Celosia argentea* Plant Extract and Their Efficacy Studies as Antioxidant, Antibacterial, Hemolytic and Catalytic Agent. *Arabian Journal for Science and Engineering*, 44(7), 6435-6444.
- Shankar S.S., Ahmed A., Akkamwar B., Sastry M., Rai A., Singh A. Biological synthesis of triangular gold nanoprisms, *Nature*, 3 482, (2004)
- Sol-Gel Science: The Physics and Chemistry of Sol-Gel Processing, ed. C. J. Brinker and G. W. Scherer, Academic Press, USA, 1990, e-book, http://depts.washington.edu/solgel/documents/class_docs/MSE502/SolGel_Science_The_physics_and_chemistry_of_sol-gel_processing_-_Brinker_1990.pdf.
- Sushma, N. J., Prathyusha, D., Swathi, G., Madhavi, T., Raju, B. D. P., Mallikarjuna, K., & Kim, H. S. (2016). Facile approach to synthesize magnesium oxide nanoparticles by using *Clitoria ternatea*—characterization and in vitro antioxidant studies. *Applied Nanoscience*, 6(3), 437-444.
- Venkatesha, T. G.; Nayaka, Y. A.; Chethana, B. K. Adsorption of Ponceau S from Aqueous Solution by MgO Nanoparticles. *Appl. Surf. Sci.* 2013, 276, 620–627. DOI: 10.1016/j.apsusc.2013.03.143.
- Wang, B.; Zhang, W.; Zhang, W.; Mujumdar, A. S.; Huang, L. Progress in Drying Technology for Nanomaterials. *Drying Technol.* 2005, 23, 7–32. DOI: 10.1081/DRT-200047900.
- Xu, J.; Xu, D.; Zhu, B.; Cheng, B.; Jiang, C. Adsorptive Removal of an Anionic Dye Congo Red by Flower-like Hierarchical Magnesium Oxide (MgO)-Graphene Oxide Composite Microspheres. *Appl. Surf. Sci.* 2018, 435, 1136–1142. DOI: 10.1016/j.apsusc.2017.11.232.